CHEMISTRY OF MATERIALS
Article

Chem. Mater. **2010,** *22,* 5129–5136 5129
DOI:10.1021/cm1006907

Monolithic Zinc Oxide Aerogels from Organometallic Sol−Gel Precursors

Michael Krumm, Carlos Lizandara Pueyo, and Sebastian Polarz*

Department of Chemistry, University of Konstanz, 78457 Konstanz, Germany

Received March 7, 2010. Revised Manuscript Received August 4, 2010

Aerogels belong to the large class of porous solids. They are characterized by a network of a mechanically stable solid, most likely inorganic in nature comprising a large gas volume in comparison to the volume of the solid material. Although a large variety of aerogels with silicate networks already exist, examples for materials with transition metal oxide networks are rare. One particularly interesting target is zinc oxide because of its semiconducting and multifunctional character. A sol−gel process facilitating an organometallic precursor system is established. The mechanism of gelation has been studied in detail. Unlike most other sol−gel processes, at first a large number of nanocrystalline ZnO particles are formed that rapidly agglomerate to secondary aggregates instead of forming a network directly. Thus, these secondary aggregates determine the textural properties of the pore walls as they assemble into the final, highly cross-linked network. A monolithic ZnO aerogel with porosities greater than 99% could be received after solvent extraction with supercritical CO_2. Furthermore, the porosities could be tuned via a combination of conventional drying and supercritical solvent extraction by a process that we call scalar drying. Finally, one of the potential functional properties of the new ZnO aerogels was proven, its application in photocatalysis.

Introduction

The gas phase and the solid state are traditionally seen as opposites. For instance the density of gases is very low ($\rho_{air} = 0.00129$ g/cm^{-3}) and those of solids is magnitudes higher ($\rho_{zinc\ oxide} \approx 4346 \times \rho_{air} = 5.606$ g/cm^3). Therefore, one would erroneously expect that it is impossible that a solid material possesses a similar density than air. Because of the compliant dimension in density, the described class of materials has been termed aerogels. Such materials are characterized by a network of a mechanically stable solid, most likely inorganic in nature comprising a large gas volume V_P in comparison to the volume of the solid material V_s. Because the volume of the entire body V_{tot} is given by the sum of V_P and V_S, the porosity defined as $P = V_P/V_{tot}$ will be 90% or even greater. Exciting examples are organosilica materials with a density of only $3\rho_{air} = 0.004$ g/cm^{-3}.[1−3]

Because of their unique structure, a range of interesting properties and applications are known for aerogels, which have also been described in several excellent review articles.[4,5] In addition to obvious applications in catalysis, in particle or protein immobilization, and sensing or separations technology,[6] aerogels are characterized by remarkably low thermal and acoustic conductivity.[7,8] A unique application was the collection of cosmic dust. The majority of known aerogels contain silica as the inorganic matrix. Because silica is electrically insulating and also somewhat restricted in catalysis, there exists a significant interest in the preparation of functional metal oxide aerogels. The first examples for alumina have been known for a long time.[9] In the meantime, vanadium oxide,[10] molybdenum oxide, manganese oxide materials have also been described.[11,12] Recently, a nice report about a CdSe areogel has been published.[11] It is surprising that despite the high relevance of zinc oxide in many fields, there is to the best of our knowledge not one single paper reporting about pure ZnO aerogels. Lorenz et al. describe a silia aerogel containing nanocrystalline ZnO particles.[13] Hupp et al. have used a similar approach. They have started from a silica gel, and they could achieve the coverage of the SiO_2 matrix with zinc oxide.[14] Hope-Weeks et al. have reported a monolithic ZnO material in 2007.[15] Although the materials have an interesting microstructure, they are very

*Corresponding author. E-mail: sebastian.polarz@uni-konstanz.de.

(1) Bourret, A. *Europhys. Lett.* **1988**, *6*, 731.
(2) Lee, K. H.; Kim, S. Y.; Yoo, K. P. *J. Non-Cryst. Solids* **1995**, *186*, 18.
(3) Tillotson, T. M.; Hrubesh, L. W. *J. Non-Cryst. Solids* **1992**, *145*, 44.
(4) Huesing, N.; Schubert, U. *Angew. Chem.* **1998**, *110*, 22.
(5) Pierre, A. C.; Pajonk, G. M. *Chem. Rev.* **2002**, *102*, 4243.
(6) Bhatia, R. B.; Brinker, C. J.; Gupta, A. K.; Singh, A. K. *Chem. Mater.* **2000**, *12*, 2434.
(7) Yoldas, B. E.; Annen, M. J.; Bostaph, J. *Chem. Mater.* **2000**, *12*, 2475.
(8) Conroy, J. F. T.; Hosticka, B.; Davis, S. C.; Smith, A. N.; Norris, P. M. *Microscale Thermophys. Eng.* **1999**, *3*, 199.
(9) Teichner, S. J.; Nicolaon, G. A.; Vicarini, M. A.; Gardes, G. E. E. *Adv. Coll. Interf. Sci.* **1976**, *5*, 245.
(10) Livage, J. *Chem. Mater.* **1991**, *3*, 578.
(11) Bag, S.; Arachchige, I. U.; Kanatzidis, M. G. *J. Mater. Chem.* **2008**, *18*, 3628.
(12) Rolison, D. R.; Dunn, B. *J. Mater. Chem.* **2001**, *11*, 963.
(13) Lorenz, C.; Emmerling, A.; Fricke, J.; Schmidt, T.; Hilgendorff, M.; Spanhel, L.; Mueller, G. *J. Non-Cryst. Solids* **1998**, *238*, 1.
(14) Hamann, T. W.; Martinson, A. B. E.; Elam, J. W.; Pellin, M. J.; Hupp, J. T. *Adv. Mater.* **2008**, *20*, 1560.
(15) Gao, Y. P.; Sisk, C. N.; Hope-Weeks, L. J. *Chem. Mater.* **2007**, *19*, 6007.

Published on Web 08/19/2010

different to classical aerogels. The mentioned materials have very large pores (~500 nm to 1 μm) and are constructed from a random assembly of large crystalline plates instead of a filigreed network.

The tremendous interest in zinc oxide is provoked by its multifunctional character. ZnO is a member of the class of II−VI semiconductors. It is a promising material for UV light-emitting-diodes (LEDs) and lasers,[16−18] solar cells,[19−21] field-emission displays, as a high-efficiency green phosphor,[22] as an UV-photodetector material,[23] as a gas-sensor,[24,25] or varistor.[26] Apart from these emerging applications it is also important in large-scale products such as catalysis (e.g., methanol synthesis over Cu/ZnO catalysts),[27−29] rubber compounding, or as an UV blocker in sun-lotions.[30] Some interesting reports have also described the photocatalytic activity of zinc oxide.[31−36] ZnO crystallizes in the Wurtzite structure and, as a consequence, is both pyroelectric and piezoelectric, which represents the basis for applications in electromechanical or thermoelectrical coupling devices.[37,38] A comprehensive description of ZnO can be found in one of the recent review articles.[39−43]

The first step in the preparation of an aerogel is the classical sol−gel process. The hydrolysis and polycondensation of appropriate precursors leads to the formation of sol particles that eventually stick to each other and form a gel.[44] When the liquid filling the pores can be removed, avoiding a phase transition, respectively a liquid−vapor interface and the resulting capillary forces, the dry gel can be obtained without shrinkage. Therefore, supercritical drying preferentially with carbon dioxide can be used for the removal of the liquid occupying the pore volume. In an ideal case, the pore structure of the aerogel is exactly the same compared to the wet state. Thus, for finding explanations why there are no reports about ZnO aerogels, one has to analyze the current state of the art in sol−gel science for zinc oxide. The sol−gel process for ZnO is much less developed and has been much less investigated in detail in comparison to silica or other transition metal oxides for instance titania (TiO_2). In most cases one uses molecular precursors like, e.g., metal alkoxides $M(OR)_x$. The advantage of using such compounds is that kinetic factors can be adjusted with high precision. However, the alkoxides of zinc $Zn(OR)_2$ are coordination polymers which are insoluble in common solvents. This is the reason why salt precursors for instance zinc acetate or zinc nitrate are commonly used when it comes to the sol−gel preparation of zinc oxide.[45−48] Typically, $Zn(OH)_2$ is formed under basic conditions followed by the dehydration resulting in ZnO. The discussed method is quite suited for the preparation of zinc oxide nanoparticles under aqueous conditions, but it is difficult to obtain continuous networks comprising an organic solvent phase.

The aims for the research work presented here can by formulated as follows: (A) The establishment of a ZnO sol−gel process leading to the reproducible formation of gels rather than particles. (B) The conversion of those gels into the first zinc oxide aerogels, and the variation of the textural properties, and exploring potential applications that benefit from the aerogel character of the ZnO materials.

Experimental Section

All starting compounds were received from Aldrich, were purified and carefully dried prior to use. $ZnMe_2$ and $[MeZnOR]_4$ heterocubanes according to methods reported in the literature.[24,28,29,49−52]

Preparation of ZnO Gels. In a typical synthesis, the used ZnO precursor was dissolved under moderate heating in diglyme ($c_{precursor}$ = 0.09 M). The solution was cooled to 0 °C and 4 equiv. of water were added. The solution was kept at 0 °C for at least 4 days, during which the gels could form. Afterward they were gradually warmed and finally kept for 3 days at 60 °C.

(16) Look, D. C.; Claftin, B. *Phys. Status Solidi B* **2004**, *241*, 624.
(17) Meyer, B. K.; Alves, H.; Hofmann, D. M.; Kriegseis, W.; Foerster, D.; Bertram, F.; Christen, J.; Hoffmann, A.; Strassburg, M.; Dworzak, M.; Haboeck, U.; Rodina, A. V. *Phys. Status Solidi B* **2004**, *241*, 231.
(18) Look, D. C.; Reynolds, D. C.; Litton, C. W.; Jones, R. L.; Eason, D. B.; Cantwell, G. *Appl. Phys. Lett.* **2002**, *81*, 1830.
(19) Martinez, M. A.; Herrero, J.; Gutierrez, M. T. *Sol. Energy Mater. Sol. Cells* **1997**, *45*, 75.
(20) Anderson, N. A.; Ai, X.; Lian, T. Q. *J. Phys. Chem. C B* **2003**, *107*, 14414.
(21) Keis, K.; Lindgren, J.; Lindquist, S. E.; Hagfeldt, A. *Langmuir* **2000**, *16*, 4688.
(22) Darici, Y.; Holloway, P. H.; Sebastian, J.; Trottier, T.; Jones, S.; Rodriquez, J. *J. Vac. Sci. Tech. A* **1999**, *17*, 692.
(23) Monroy, E.; Omnes, F.; Calle, F. *Semicond. Sci. Technol.* **2003**, *18*, R33.
(24) Polarz, S.; Roy, A.; Lehmann, M.; Driess, M.; Kruis, F. E.; Hoffmann, A.; Zimmer, P. *Adv. Funct. Mater.* **2007**, *17*, 1385.
(25) Lin, H. M.; Tzeng, S. J.; Hsiau, P. J.; Tsai, W. L. *Nanostruct. Mater.* **1998**, *10*, 465.
(26) Clarke, D. R. *J. Am. Ceram. Soc.* **1999**, *82*, 485.
(27) Peppley, B. A.; Amphlett, J. C.; Kearns, L. M.; Mann, R. F. *Appl. Catal., A* **1999**, *179*, 21.
(28) Polarz, S.; Strunk, J.; Ischenko, V.; Van den Berg, M.; Hinrichsen, O.; Muhler, M.; Driess, M. *Angew. Chem.* **2006**, *118*, 3031.
(29) Polarz, S.; Neues, F.; Van den Berg, M.; Gruenert, W.; Khodeir, L. *J. Am. Chem. Soc.* **2005**, *127*, 12028.
(30) Fan, J.; Freer, R. *J. Appl. Phys.* **1995**, *77*, 4795.
(31) Wang, J.; Liu, P.; Fu, X.; Li, Z.; Han, W.; Wang, X. *Langmuir* **2008**, *25*, 1218.
(32) Morrison, S. R.; Freund, T. *J. Chem. Phys.* **1967**, *47*, 1543.
(33) Miyauchi, M.; Nakajima, A.; Watanabe, T.; Hashimoto, K. *Chem. Mater.* **2002**, *14*, 2812.
(34) Pal, B.; Sharon, M. *Mater. Chem. Phys.* **2002**, *76*, 82.
(35) Daneshvar, N.; Salari, D.; Khataee, A. R. *J. Photochem. Photobiol., A* **2004**, *162*, 317.
(36) Yang, J. L.; An, S. J.; Park, W. I.; Yi, G. C.; Choi, W. *Adv. Mater.* **2004**, *16*, 1661.
(37) Look, D. C. *Mater. Sci. Eng., B* **2001**, *80*, 383.
(38) Hickerne *IEEE Trans. Microwave Theory Tech.* **1969**, *MT17*, 957.
(39) Wang, Z. L. *J. Phys. Condens. Matter* **2004**, *16*, R829.
(40) Ozgur, U.; Alivov, Y. I.; Liu, C.; Teke, A.; Reshchikov, M. A.; Dogan, S.; Avrutin, V.; Cho, S. J.; Morkoc, H. *J. Appl. Phys.* **2005**, 98.
(41) Klingshirn, C. *Phys. Status Solidi B* **2007**, *244*, 3027.
(42) Klingshirn, C. *Chemphyschem* **2007**, *8*, 782.
(43) Woell, C. *Prog. Surf. Sci.* **2007**, *82*, 55.
(44) Brinker, C. J.; Scherer, G. W. *Sol−Gel Science: The Physics and Chemistry of Sol−Gel Processing*, 1st ed.; Academic Press: London, 1990.
(45) Kamalasanan, M. N.; Chandra, S. *Thin Solid Films* **1996**, *288*, 112.
(46) Meulenkamp, E. A. *J. Phys. Chem. C B* **1998**, *102*, 5566.
(47) Natsume, Y.; Sakata, H. *Thin Solid Films* **2000**, *372*, 30.
(48) Lee, J. H.; Ko, K. H.; Park, B. O. *J. Cryst. Growth* **2003**, *247*, 119.
(49) Ischenko, V.; Polarz, S.; Grote, D.; Stavarache, V.; Fink, K.; Driess, M. *Adv. Funct. Mater.* **2005**, *15*, 1945.
(50) Polarz, S.; Orlov, A.; Van den Berg, M.; Driess, M. *Angew. Chem., Int. Ed.* **2005**, *44*, 7892.
(51) Polarz, S.; Roy, A.; Merz, M.; Halm, S.; Schröder, D.; Scheider, L.; Bacher, G.; Kruis, F. E.; Driess, M. *Small* **2005**, *1*, 540.
(52) Lizandara-Pueyo, C.; van den Berg, M.; de Toni, A.; Goes, T.; Polarz, S. *J. Am. Chem. Soc.* **2008**, *130*, 16601.

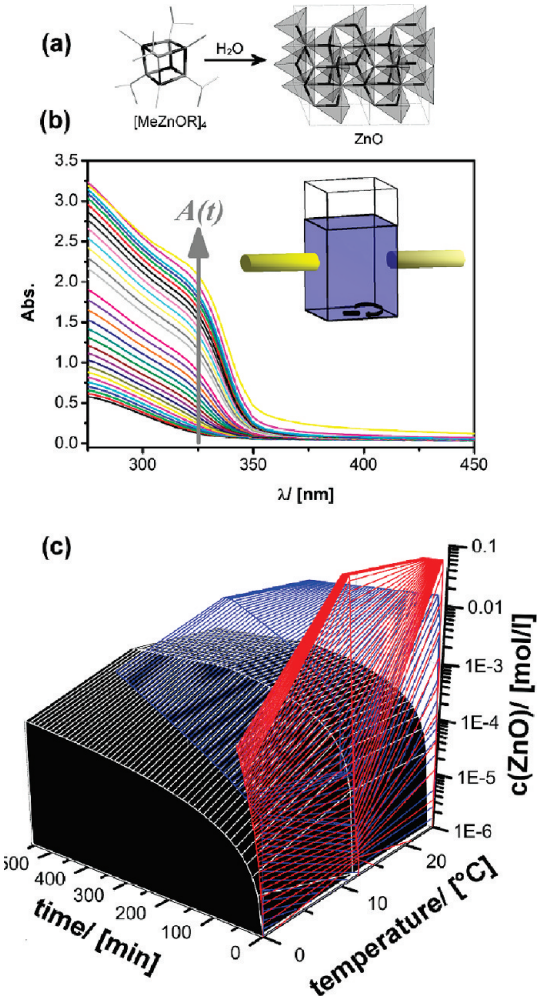

Figure 1. Formation of ZnO from the reaction of the organometallic heterocubane precursor with water (a) can be monitored as a function of time via the emergence of the adsorption edge in UV/vis transmission spectra (b). Influence of the process temperature and the precursor concentration ($c = 1 \times 10^{-3}$ mol/L ⟷ black surface; $c = 1 \times 10^{-2}$ mol/L ⟷ blue surface; $c = 7.2 \times 10^{-2}$ mol/L ⟷ red surface) on the formation of ZnO (plotted as c(ZnO)).

Drying of ZnO Gels. Conventional drying was accomplished in an oil-pump vacuum at 50 mbar under heating to 50 °C. For supercriticial drying, the as-prepared aerogels placed into a stainless-steel autoclave. First, the pore liquid was exchanged with liquid CO_2 at ~60 bar for 4 days under daily exchange with new CO_2. Afterward the temperature and pressure was ramped above the critical point of CO_2 and kept there for another 2 days. The supercritical fluid was released within 2 h.

Testing of the Photocatalytic Activity. The photocatalytic investigations were performed according to procedures described in the literature.[31−36] The photocatalytic activity of zinc oxide with aerogel character was investigated by the photodegradation of Rhodamine B at room temperature. The ZnO material (50 mg) was dispersed in an aqueous solution of Rhodamine B ($c = 2 \times 10^{-5}$ mol/L; 50 mL). Before irradiation the dispersion was stirred in the dark for 3 h to establish an adsorption−desorption equilibrium at the surface of the catalyst. Then, the mixture was placed in a distance of 10 cm in front of a UV-light source (TQ 150, Heraeus,150W). Samples were taken and filtered through a 200 nm syringe filter to remove the ZnO material. The remaining concentration of Rhodamine B was determined using UV−vis spectroscopy

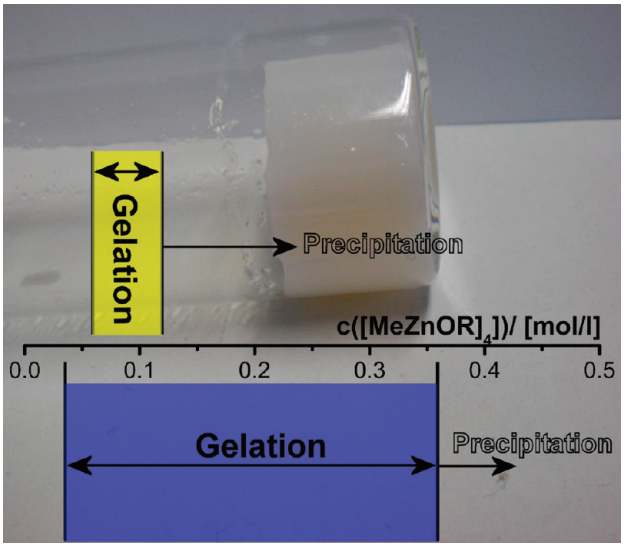

Figure 2. Photographic image of a wet ZnO gel and the concentration range for which gelation occurs. Yellow area: $[MeZnO^{iso}Pr]_4$ as a precursor. Blue area: $[MeZnOEtOMe]_4$[29] as a precursor.

using Lambert−Beers law. The whole procedure was repeated for three cycles.

Analytic Techniques. NMR spectra were acquired on a Varian Unity INOVA 400 spectrometer. MAS NMR spectra were acquired on a Bruker DRX 400 Spektrometer. X-ray diffraction was performed on a Bruker AXS D8 Advance diffractometer using $Cu_{K\alpha}$ radiation and a Bruker AXS Sol-X solid-state energy-dispersive detector position. The UV/vis measurements were done on a Varian Cary 100 scan UV/vis spectrophotometer. The DLS experiments were performed on a Viscotek 802DLS with a coolable sample chamber using the same concentrations and conditions like in the described synthesis. TEM images were acquired on a Zeiss Libra 120 at 120kv acceleration voltage. The TEM samples were prepared by dropping a drop of the reaction solution on a carrier covered with a carbon foil (Plano company, S160A3). SEM images were recorded on a Zeiss CrossBeam 1540XB scanning electron microscope. For physisorption measurements a Micromeritics TriStar Surface and Porosity analyzer was used.

Results and Discussion

3.1. ZnO Sol−Gel Process. For some time our group has been concerned with a special class of organometallic zinc-oxo precursors. Unlike others like, for instance, Chaudret et al., who have used sources like dialkylzinc (e.g., $ZnEt_2$) for the preparation of ZnO colloids of amazing quality,[53−56] the character of our precursor system is between such purely organometallic compounds and the aforementioned zinc-bis-alkoxides. Tetrameric alkylzincalkoxides featuring a heterocubane architecture have proven to be of extraordinary value for the preparation of various ZnO materials.[24,28,29,49−52] Recently, the

(53) Rataboul, F.; Nayral, C.; Casanove, M. J.; Maisonnat, A.; Chaudret, B. *J. Organomet. Chem.* **2002**, *643*, 307.
(54) Monge, M.; Kahn, M. L.; Maisonnat, A.; Chaudret, B. *Angew. Chem., Int. Ed.* **2003**, *42*, 5321.
(55) Kahn, M. L.; Monge, M.; Colliere, V.; Senocq, F.; Maisonnat, A.; Chaudret, B. *Adv. Funct. Mater.* **2005**, *15*, 458.
(56) Kahn, M. L.; Cardinal, T.; Bousquet, B.; Monge, M.; Jubera, V.; Chaudret, B. *Chemphyschem* **2006**, *7*, 2392.

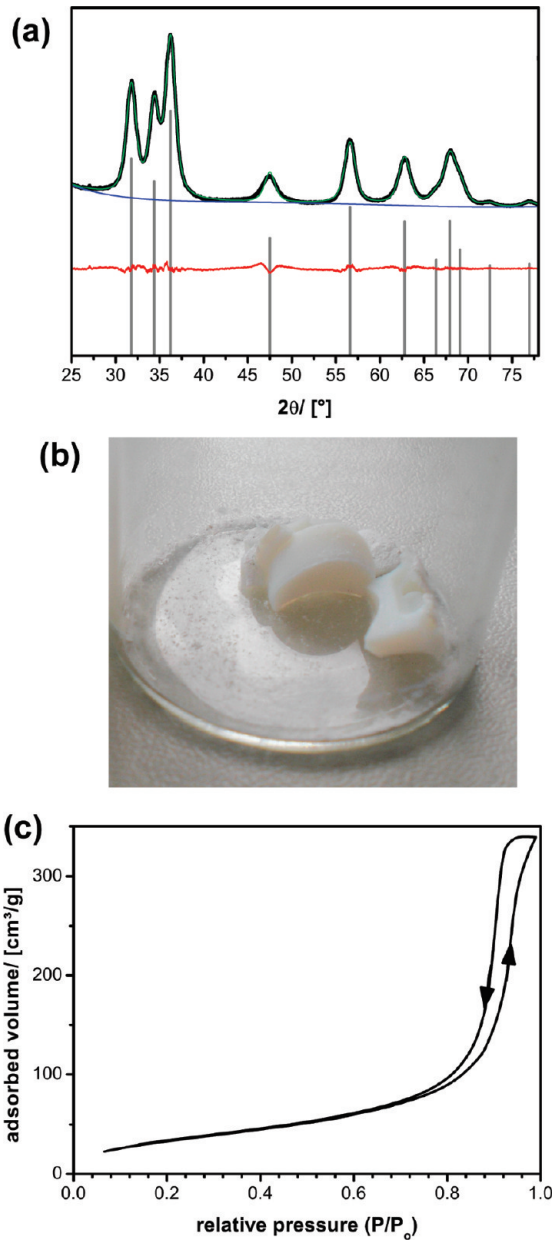

Figure 3. (a) PXRD data of the ZnO materials obtained after conventional drying of the wet gels; black ≅ experimental data; green ≅ Warren-Averbach Le-Bail fit; red ≅ difference; blue ≅ background; gray ≅ reference pattern of bulk ZnO. (b) Photographic image and (c) N_2-physisorption data of the aerogel.

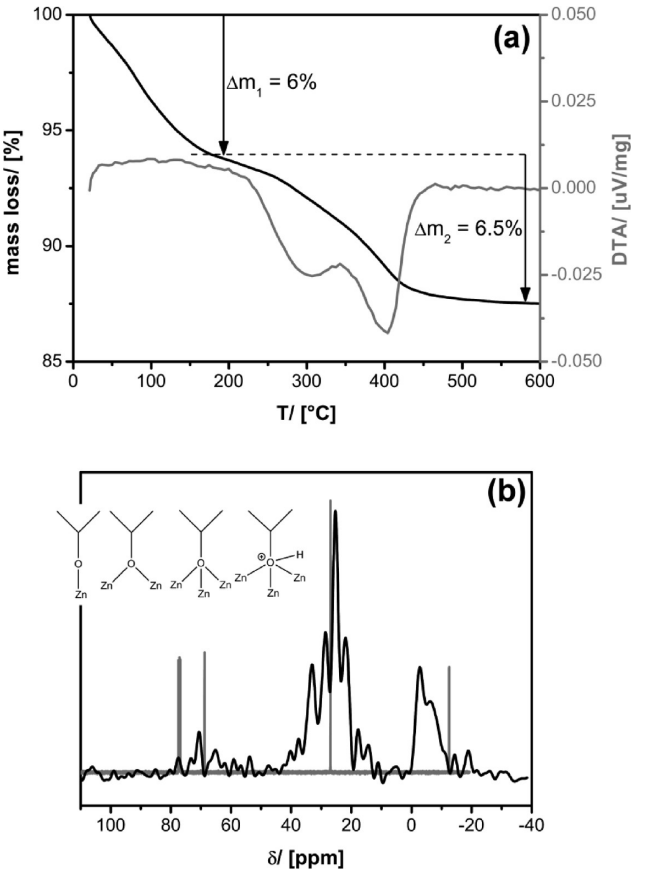

Figure 4. (a) TGA and DTA data of the ZnO materials obtained after conventional drying of the wet gels. (b) Solid-state ^{13}C NMR data of the solid material in comparison to the spectrum of the precursor $[MeZnO^{iso}Pr]_4$ (gray, recorded in $CDCl_3$) as a reference. Reasonable alternatives for the surface coordination of the isopropoxy groups are also shown.

nucleation and growth of crystalline ZnO particles originating from the reaction of the $[MeZnOR]_4$ with water has been investigated in detail using several in situ methods.[52]

Because the band gap of ZnO is $\Delta E = 3.3$ eV, its formation starting from a homogeneous solution of the precursor $[MeZnOR]_4$ in an organic solvent (Figure 1a) induces the emergence of an absorption edge (see Figure 1b) which can be used to follow the ongoing reaction directly and with a relatively good time resolution. The measurements were performed in transmission mode, which is possible because the particles form in homogeneous solution. The results are reliable when there is only minor scattering, for example, due to very large particles (size >200 nm). Because the sol obtained in our experiments contains nanoscaled particles (<50 nm) for a significant time, effects originating from scattering can be ignored. Then, the absorption value $A(t)$ can be used to determine the concentration of ZnO at each moment using Labert−Beers law

$$A(t)_{\lambda = 325\ \mathrm{nm}} = \varepsilon_{\lambda = 325\ \mathrm{nm}} C_{\mathrm{ZnO}}(t) d \qquad (1)$$

with $\varepsilon_{\lambda = 325\ \mathrm{nm}} \cong$ the extinction coefficient at $\lambda = 325$ nm, and $d \cong$ the inner extension of the cuvette = 10.000 mm. The rate of ZnO formation is influence by changing the alkoxide group (Me > Et > Pr > iso-Pr > Bu ≈ OEtOMe > tert-Bu),[52] the temperature or the precursor concentration (see Figure 1c). The role of the latter two parameters has been extensively studied. The results are shown in Figure 1c. As expected an increase of temperature leads to an increase of the rate of ZnO formation. The influence of the precursor concentration is also pronounced. The detailed investigation has been proven to be very important in controlling the gelation processes. There is a certain point when at low temperature the reaction proceeds very slowly (Figure 1b). The precipitation of irregular agglomerates then becomes the dominant process but the entire system starts to gel (see Figure 2). It is important to note that an entirely different material can be obtained from the same precursor system when the ZnO particles emerging under kinetically controlled conditions are stabilized as colloids

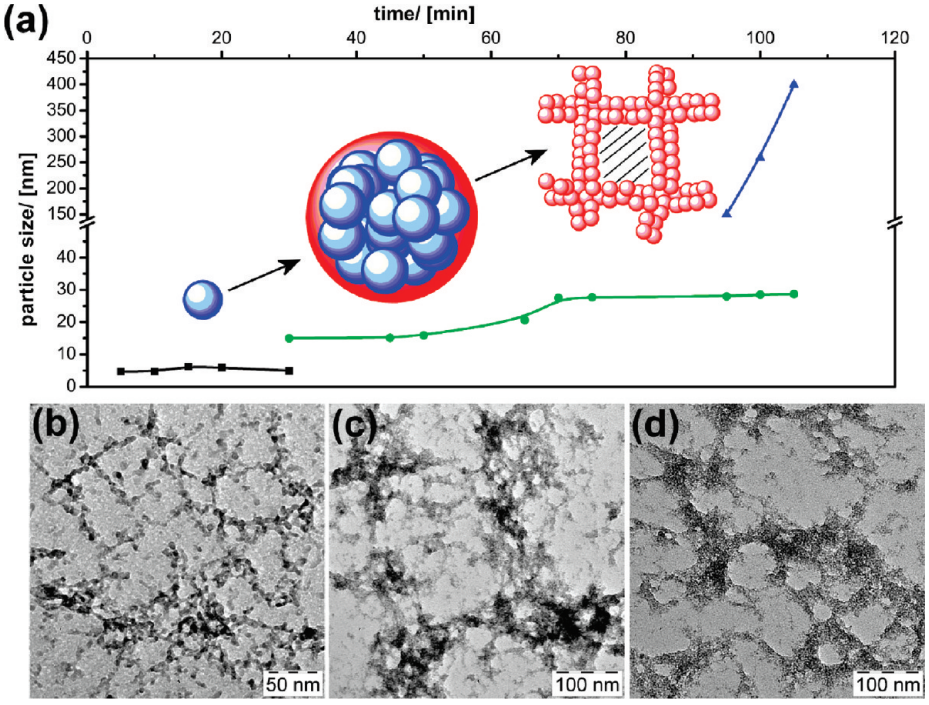

Figure 5. (a) Particle size as a function of reaction time as determined by DLS measurements. The mechanism of gel formation is shown schematically. It proceeds from the primary particles (data points ≅ black squares) to secondary agglomerates (green spheres) and finally to the tertiary gel structure (blue triangles). TEM micrographs of samples taken at t = (b) 13, (c) 90, and (d) 131 min.

during their growth phase. A recent publication describes the formation of metastable particles stabilized by polyvinyl pyrrolidone comprising the novel ZnO with alpha-boron nitride structure.[57] In the current study, there is no agent for colloidal stabilization present. Thus, the particles possess the conventional Wurtzite structure, but because of their agglomeration to networks, they form a new material, the ZnO aerogels described here. Likewise, it has been observed that also precursor concentration and heterocubane type are of importance. This is not surprising since also these two factors influence the ZnO formation rate as discussed above. There are only more or less narrow regions of concentration in which the gelation is successful. This region is much wider for $[MeZnOEtOMe]_4$ in comparison to $[MeZnO^{iso}Pr]_4$ (see Figure 2). Outside these regions, it comes to precipitation of ZnO agglomerates, which have already been described in a previous publication.[52] A typical gel contains of the order of ~165 mL solvent per gram of solid material. This indicates a porosity of more than ~99%. Because it is difficult to analyze the wet gels directly, the pore solvent was removed to begin with by drying of the wet gels in oil-pump vacuum. A strong decrease in volume accompanied the removal of the pore liquid, but the materials retain their monolithic structure (see Figure 3b). This is quite unusual because most wet gels lose their structure when dried conventionally because the capillary forces induce a collapse of the pore system.[4] The materials contain ZnO in the Wurtzite modification as the only crystalline phase according to powder X-ray diffraction (PXRD) shown in Figure 3a. The single reflexes are very broad indicating that the particle size is in the nanodomain. The average particle size is 6.9 nm according to a full profile analysis using a Warren−Averbach Le Bail fit (Figure 3a). From now on, the mentioned particles will be denominated "primary particles". It is interesting to note that the size of the primary particles remains almost unaffected by changes in reaction parameters like precursor concentration, amount of water added, etc. (see the Supporting Information, SI-1). The surface area of the materials determined from BET evaluation of N_2 physisorption data (Figure 3c) is of the order of 130−150 m^2/g. A BJH pore-size distribution analysis of the isotherms (shown in the Supporting Information, SI-3,) shows a maximum at 32 nm.[58] The latter data indicate that even under conditions of conventional drying, a highly (meso-)porous material with well-accessible primary particles remains stable.

Because PXRD is sensitive only toward the crystalline parts of a sample, additional analytical techniques have been applied. Thermogravimetric and differential thermoanalysis data are shown in Figure 4a. A continuous, endothermic mass loss is observed from room temperature until ~170 °C that can be attributed to the evaporation of residual solvent and water entrapped in the porous ZnO matrix. Two exothermic processes occur at T = 303 and 402 °C. The associated mass loss (Δm = 6.5%) originates from more strongly bound organic species. The chemical nature of those groups was investigated by FT-IR- and solid-state NMR spectroscopy. Solid-state ^{13}C NMR spectra were acquired (Figure 4b). Despite the long acquisition times (~1 week), because of the low amount of organics and because the significant porosity of the

(57) Pueyo, C. L.; Siroky, S.; Landsmann, S.; van den Berg, M. W. E.; Wagner, M. R.; Reparaz, J. S.; Hoffmann, A.; Polarz, S. *Chem. Mater.* **2010**, *22*, 4263.

(58) Barret, E. P.; Joyner, L. G.; Halenda, P. H. *J. Am. Chem. Soc.* **1951**, *73*, 373.

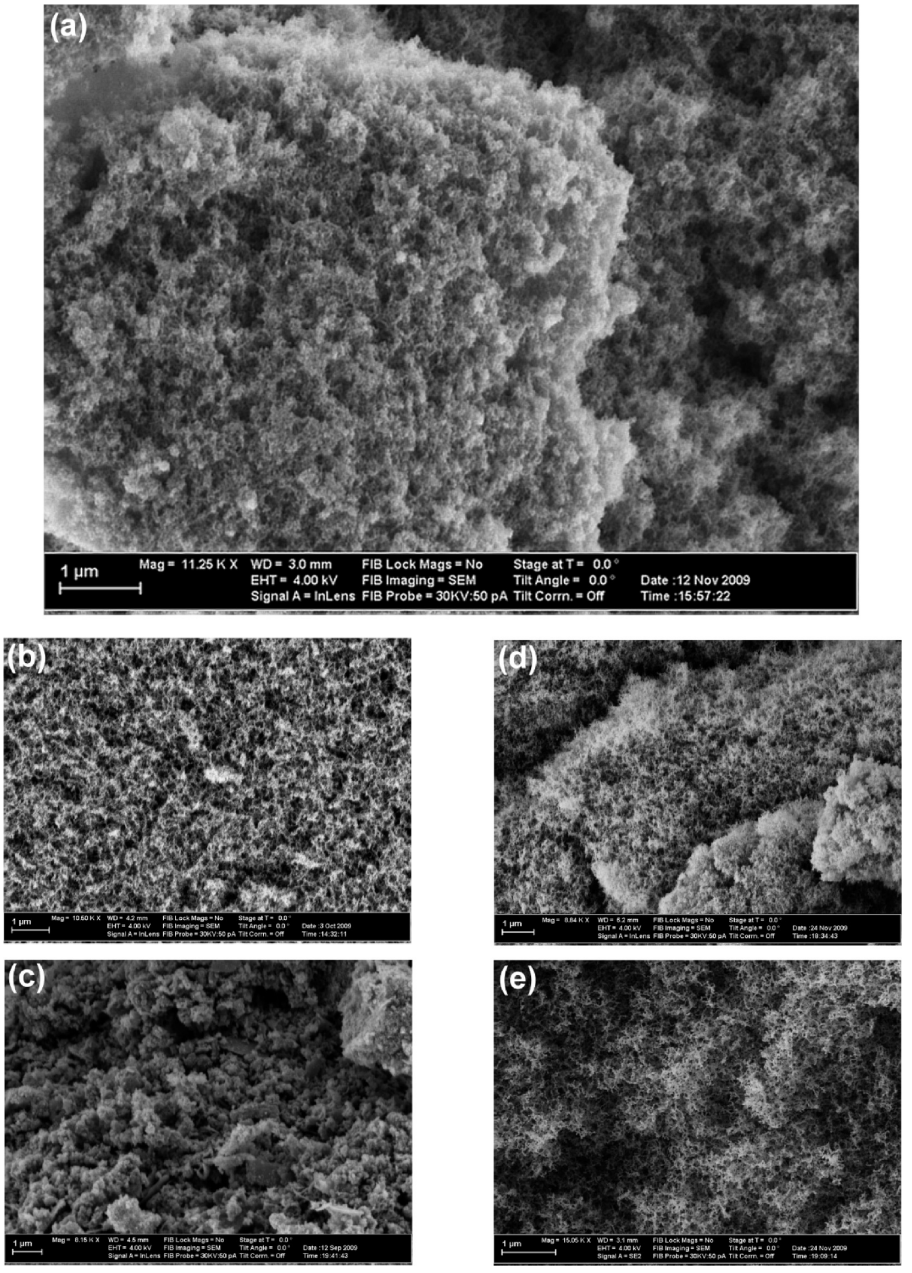

Figure 6. SEM image of the ZnO aerogels obtained after direct supercritical extraction of the as prepared wet gel (a). Aerogels obtained via gradual drying followed by supercritical extraction: (b) partially dried, (c) fully dried. Aerogels obtained via solvent exchange in the wet state followed by supercritical extraction with (d) toluene and (e) hexane.

samples the signal-to-noise ratio was still relatively low. However, three regions could be clearly identified where signals occur. The direct comparison to the ^{13}C NMR spectrum of the precursor $[MeZnO^{iso}Pr]_4$ indicates that the signal group at $\delta \approx 71$ ($O\underline{C}H(CH_3)_2$) and 33−21 ppm ($OCH(\underline{C}H_3)_2$) originate from iso-propoxy groups bound in different coordination modes to the surfaces of the ZnO particles (Figure 4b). An additional signal at $\delta \approx -3$ ppm is present in the spectrum. The latter signal can only be explained by residual "$H_3\underline{C}-Zn-O-(ZnO)_\infty$" groups at the surfaces. The occurrence of the latter species is unexpected because the gels were prepared in the presence of water. To check that the observed signals were not caused by any residual, nonreacted molecular precursor compounds soxhleth extraction with pentane was adopted to the materials for three days, and solid-state ^{13}C NMR spectra were measured again. Because the mentioned signals were still present, it is proven that the corresponding functional groups are chemically bound to the ZnO network. Our results indicate that the groups located at the surface of the ZnO materials originate directly from the precursor compound. The organic surface groups obviously play a crucial role regarding the colloidal stabilization of the inorganic particles during the sol−gel process considering the quite different gelation regions for $[MeZnO^{iso}Pr]_4$ in comparison to $[MeZnOEtOMe]_4$ (Figure 2).

The formation of the gel was investigated in detail using dynamic light scattering measurements (DLS) and transmission electron microscopy measurements (TEM) of

samples taken directly from the reaction system. Immedeately after the start of the reaction, during the first 30 min a large number of particles in the size range ~6 nm form (see Figure 5a,b). Considering the previous findings from PXRD, it can be concluded that these represent the nanocrystalline primary particles. In the course of time, the concentration of the primary particles increases, and the chances for collisions between them is enhanced. This leads to the formation of agglomerates of steadily growing size (Figure 5a,c). When these agglomerates have reached a size of ~20−30 nm (at $t \approx 75$ min), all primary particles have been consumed. The dispersions are stable for an additional period of ≈20 min. Eventually the secondary particles form a network leading to strongly growing structures. Already, 10 min later, the structures became too large to be observable by our DLS equipment. However, TEM data (Figure 5b−d) support nicely the proposed mechanism that involves three well-differentiable steps (Figure 5a): The formation of nanocrystalline primary particles, followed by their assembly into secondary agglomerates. The latter species forms the final, tertiary gel structure.

3.2. ZnO Aerogels. The wet gels were transferred into an autoclave and the pore liquid was exchanged with supercritical CO_2 using the setup shown in the Supporting Information, SI-2. The particular advantage of this setup is that a continuous removal of the pore liquid is possible. Bulky monolithic bodies possessing almost the same volume than the wet gels have been obtained after the supercritical fluid was released. The structure of the resulting materials was studied using scanning electron microscopy SEM (see Figure 6a). The transformation of the wet gel into the first ZnO aerogel has obviously been successful.

An extremely porous and homogeneous material can be seen. A SEM image taken at higher magnification shows very well the structure of the ZnO network (see the Supporting Information, SI-3). The structure of the aerogels as well as the mechanism proposed for their formation (Figure 5) could be supported by TEM measurements shown in Figure 7. It can be seen very nicely how the network of the secondary aggregates forms a porous structures with irregular pores in the range ~30−100 nm. The thickness of the pore walls is determined by the size of the secondary aggregates composed of the primary particles.

The next task was to explore possibilities for changing the textural parameters of the aerogels. It was mentioned before that the conventional drying does not lead to powdered xerogels but to monolithic samples, and that the surface area of such materials is still very high. Therefore, materials with different porosities could be prepared if the conventional drying is interrupted at a certain point and the remaining pore liquid is removed by extraction with supercritical CO_2. It can be seen that the volume of such monoliths gradually decreases (see the photographs in the Supporting Information, SI-4). The change in volume has also consequences for the microstructure of the aerogels. The porous solids become more and more compact (Figure 6a−c). Interestingly, the exchange of the solvent in the wet gel state has a totally different but not less pronounced effect. Also in this case it was possible to study the effect by SEM of the supercritically dried aerogels (Figure 6d,e). The change of solvent from diglyme used during the synthesis (see Experimental Section) to less polar solvents leads to a significant reconstruction of the entire network. For toluene (Figure 6d) this reconstruction is less pronounced that for hexane (Figure 6e).

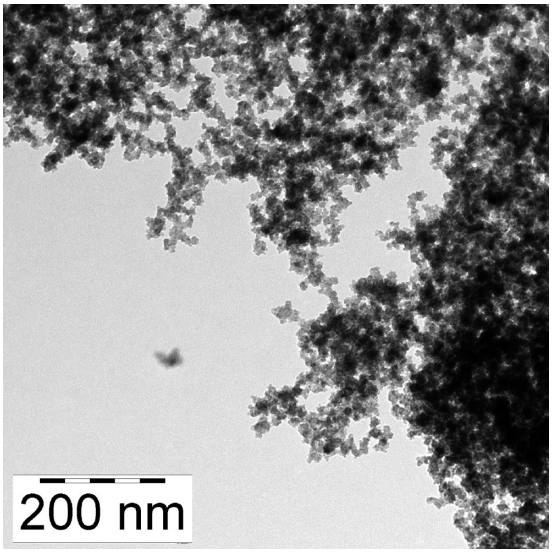

Figure 7. TEM image of a ZnO aerogel.

Recently, numerous reports have described that also ZnO materials with large internal surface are promising materials in photocatalysis.[31] We have tested the abilities of one representative ZnO aerogel material presented in the current manuscript regarding its property in the photocatalytic degradation of the dye Rhodamine B. A commercially available ZnO powder and the system containing no photocatalyst were used as references. The degradation of Rhodamine B can be followed by UV/vis spectroscopy (see the Supporting Information, SI-5). The concentration of Rhodamine B could be determined from Lambert−Beer law. Figure 8 shows the time dependency of this concentration. It is seen that there is a large difference between the three systems. The experimental data points were additionally fitted assuming an exponential decay curve: $c(t) = c_{t=0}\exp(-kt)$, with $c \cong$ the concentration of Rhodamine B, $t \cong$ time. The decay constant is $k = 1.37 \times 10^{-4}$ s^{-1} for the situation when no photocatalyst is present. For the commercially available ZnO powder $k = 2.8 \times 10^{-3}$ s^{-1} was found. The superior performance of the ZnO aerogel as a photocatalyst is reflected in significantly higher value for $k = 2.03 \times 10^{-2}$ s^{-1}. The long-term stability of the aerogel materials was tested by reusing the respective materials three times. The results of the two additional photocatalytic cycles are also shown in Figure 8. It is seen that there is practically no decrease in photocatalytic activity. The latter observation fits to the fact that there was no structural change in aerogel character detected by SEM

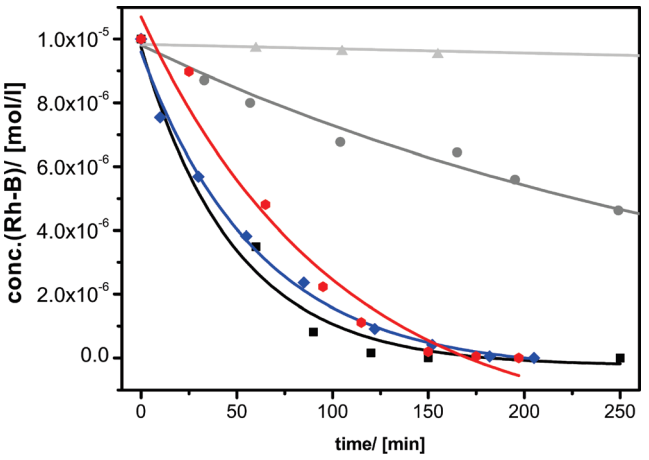

Figure 8. Photocatalytic degradation of rhodamine B determined by UV−vis spectroscopy. Points: Experimental data. Solid-lines: Exponential decay function as a fit. Light gray: No photocatalyst present. Dark gray: Commercial ZnO powder as a reference catalyst. A ZnO aerogel as the photocatalyst first cycle (black), second cycle (blue), third cycle (red).

measurements, shown in the Supporting Information, SI-6. The prepared ZnO aerogel materials possess a very good structural stability.

Conclusion

One of the obstacles for the preparation of highly porous ZnO networks comprising an organic solvent that can be removed by supercritical extraction is that the current sol−gel methods for zinc oxide involve ionic precursors. Although these approaches are quite suited for the generation of ZnO nanoparticles, the ligation of the entire sol is very difficult. A sol−gel process using special organometallic ZnO precursors $[MeZnOR]_4$ could be established in the current paper. A parameter window was indentified in which gelation was successful. The control over kinetic factors of ZnO growth was a key factor. The gelation mechanism was investigated in detail. It could be shown that the process includes three steps. Initially, nanocrystalline ZnO particles with a diameter of 5−6 nm form. These particles do not directly form a network, but at first larger particulate agglomerates with a size of ~40 nm have been found. The colloidal stability of those secondary particles if influenced by surface bound organic groups originating from the molecular precursor. Surprisingly, not only alkoxide groups OR but also reactive ZnMe groups were observed. The latter result is also interesting because one can image that the latter groups could be used for the tailor-made surface modification of the materials. The described aspect is beyond the scope of the current manuscript and will be described elsewhere.

The pore liquid in the macrocopic, wet gels could be successfully removed by supercritical extraction with CO_2. The first nanocrystalline ZnO aerogel with porosities above 99% has been prepared. Two approaches were successfully applied for altering the textural properties of the zinc oxide aerogels. A postpreparative exchange of the pore liquid led to remarkable restructuring processes of the network. In addition, it was observed that the conventional drying of the wet gels, unlike to many comparable systems in the literature, does not lead to a collapse of the material. The shrinking of the materials proceeds gradually while maintaining the monolithic structure as well as the porous microstructure. Interrupting the conventional drying, followed by supercritical extraction enabled us to prepare ZnO aerogels with a systematic variation in microstructure. Finally, it was shown that the prepared materials are interesting for applications for instance in photocatalysis.

Acknowledgment. The Deutsche Forschungsgemeinschaft is acknowledged for funding (project PO780/4-1). We thank Prof. M. Antonietti for the donation of the equipment for supercritical drying.

Supporting Information Available: SI-1, effect of parameter variation on the size of the primary particles. SI-2, setup used for the preparation of the aerogels via solvent exchange with supercritical CO_2. SI-3, additional analytical data of ZnO aerogels. SI-4, gradual drying. SI-5, degradation of rhodamine B using an ZnO aerogel as a photocatalyst. SI-6, SEM images of a ZnO aerogel prior to and after 3 photocatalytic runs.This material is available free of charge via the Internet at http://pubs.acs.org.